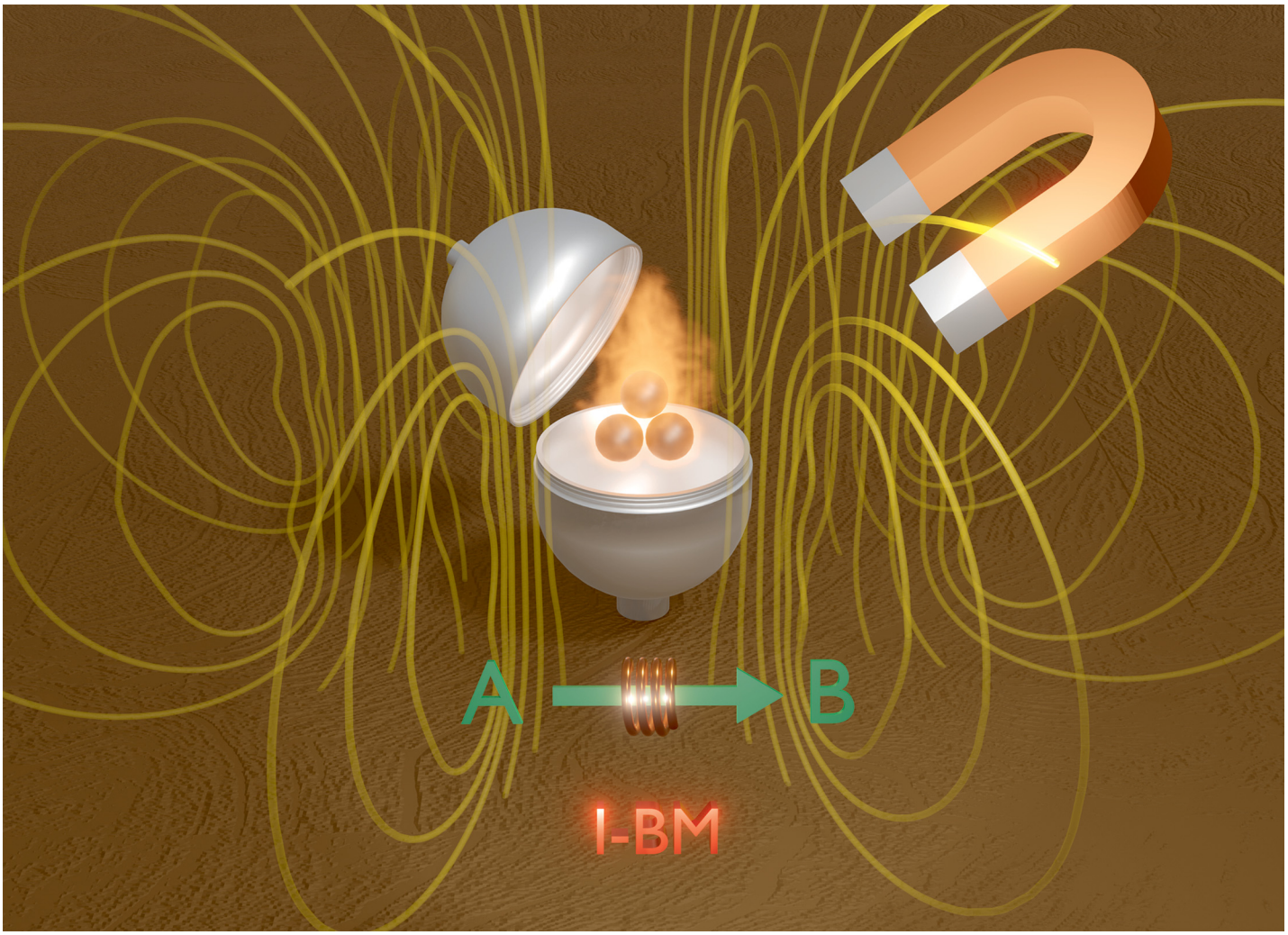

Showcasing research led by Drs Félix and Laurencin at the Institut Charles Gerhardt, CNRS, Montpellier, France.

Induction-heated ball-milling: a promising asset for mechanochemical reactions

Through a collaborative investigation performed at the CNRS in Montpellier, involving both experiments and numerical simulations, we were able to show how induction-assisted heating can be used to tune the outcome of ball-milling reactions. Depending on the choice of the materials composing the jar and beads, it is possible to heat either the walls of the jars, or the beads themselves. Examples of applications are provided, for the elucidation of reaction mechanisms, the synthesis of new molecules, and the control the physical aspect of milling media.

As featured in:

See Gautier Félix, Danielle Laurencin *et al.*, *Phys. Chem. Chem. Phys.*, 2023, **25**, 23435.

ROYAL SOCIETY OF CHEMISTRY

rsc.li/pccp

Registered charity number: 207890

PCCP Owner Societies

PCCP

PAPER

View Article Online
View Journal | View Issue

Cite this: *Phys. Chem. Chem. Phys.*, 2023, **25**, 23435

Induction-heated ball-milling: a promising asset for mechanochemical reactions†

Gautier Félix, * Nicolas Fabregue, César Leroy, Thomas-Xavier Métro, Chia-Hsin Chen ‡ and Danielle Laurencin *

Received 1st June 2023,
Accepted 11th July 2023

DOI: 10.1039/d3cp02540c

rsc.li/pccp

While ball-milling is becoming one of the common tools used by synthetic chemists, an increasing number of studies highlight that it is possible to further expand the nature and number of products which can be synthesized, by heating the reaction media during mechanochemical reactions. Hence, developing set-ups enabling heating and milling to be combined is an important target, which has been looked into in both academic and industrial laboratories. Here, we report a new approach for heating up reaction media during ball-milling reactions, using induction heating (referred to as i-BM). Our set-up is attractive not only because it enables a very fast heating of the milling medium (reaching ≈80 °C in just 15 s), and that it is directly adaptable to commercially-available milling equipment, but also because it enables heating either the walls of the milling jars or the beads themselves, depending on the choice of the materials which compose them. Importantly, the possibility to heat a milling medium "from the inside" (when using for example a PMMA jar and stainless steel beads) is a unique feature compared to previously proposed systems. Through numerical simulations, we then show that it is possible to finely tune the properties of this heating system (*e.g.* heating rate and maximum temperature reached), by playing with the characteristics of the milling system and/or the induction heating conditions used. Lastly, examples of applications of i-BM are given, showing how it can be used to help elucidate reaction mechanisms in ball-milling, to synthesize new molecules, and to control the physical nature of milling media.

Introduction

In recent years, there has been an increasing interest and enthusiasm for mechanochemistry, *i.e.* a field of chemistry that studies chemical reactions and transformations under the action of mechanical forces.[1] Notably, synthetic techniques like ball-milling, in which reagents are mixed and transformed mostly in the solid state under the action of beads, have drawn the attention not only of materials chemists, but also and more recently of molecular chemists.[2,3] Indeed, several aspects of mechanochemistry render these reactions very attractive, including (i) the total absence or very small amounts of solvents used (making it a green synthetic approach),[4] (ii) the generally increased reaction rates and yields, and (iii) the possibility to prepare new molecules and materials, which could not have been accessed nor isolated under standard synthetic conditions in solution.[5] Among relevant examples of major achievements in ball-milling syntheses, one can cite the tailored preparation of mixed-metal MOFs (metal–organic frameworks),[6] the elaboration of supramolecular Pt-square complexes for targeting guanine quadruplex motifs,[7] the preparation of gold nanoparticles,[8] and the synthesis of complex organic molecules, including π-conjugated fluorophores[9,10] and peptides.[11]

While most ball-milling reactions are performed in absence of external heating, the movements of the beads are accompanied by impacts and frictional forces, which cause an increase in temperature within the reactor.[12,13] The extent of heat generated depends on both the milling conditions and the reagents involved.[12,14,15] For example, a temperature rise of ≈7–10 °C has been measured during the simple ball-milling of pure quartz or terephthalic acid for 15 minutes.[12,14] Such an increase in temperature, in conjunction with the highly efficient mixing of the reagents, has been shown to be beneficial to help overcome the activation energy for some chemical reactions, and/or help accelerate their kinetics.[16,17] Moreover, it was shown that by pre-heating the milling jars prior to the milling, it is also possible to change the kinetics and selectivity of

ICGM, CNRS, Université de Montpellier, ENSCM, Montpellier, France.
E-mail: gautier.felix@umontpellier.fr, danielle.laurencin@umontpellier.fr

† Electronic supplementary information (ESI) available: This version contains supplementary materials, regarding the mechanochemistry and induction heating set-up, the numerical simulations and the synthetic details of the reactions. A short video illustrating the impact of inductive heating on 'snow-balls' formation is also provided. See DOI: https://doi.org/10.1039/d3cp02540c

‡ Current affiliation: Johnson Matthey Technology Centre, Blount's Court, Sonning Common, Reading, RG4 9NH, UK

Table 1 Representation of the different heating methods proposed for heating standard ball-milling systems (for a more complete literature survey, see Table S5, in ESI). Heating methods were separated depending on the presence of a direct contact between the heating source and the jar ("contact heating"), or on its absence ("contactless heating")

	CONTACT HEATING		CONTACTLESS HEATING		
	Heating system wrapped around the jar.	Heated fluid circulating around the jar.	Heat-gun pointing to the jar.	Furnace (with jar placed in it).	Induction heating (heating of the jar *or* beads).
Description of the system	Heating bands, tape, sleeves, belts, or pads (with electric connections)	Double walled jar (or beaker), or specific set-up (*e.g.* Retsch MM500)	Standard heat-gun, placed at a set distance from the jar	Furnace (incl. with specific design, adapted to the jar)	External or internal heating (depending on the jar and beads' composition)
Scheme of the heating system		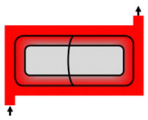	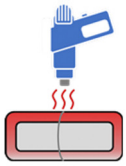	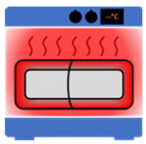	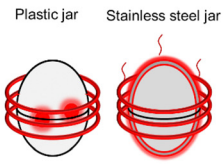
References	15,17,19–22,25,27,29,30	23,24,35–38	10,26,27,39–43	44,45	This work
Max. temp. tested	250°C		160 °C		100°C
Advantages	√ Good temp. control √ Possibility to do heating cycles with different high-temp. plateaus (esp. for heating sleeves) √ One apparatus commercially available (Retsch MM500) √ Adaptable to *operando analysis* through specific jar designs		√ Moderate to good temp. control √ Relatively simple set-up in the case of the heat-gun		√ Good temp. control √ External or internal heating (by heating the jar or the beads) √ Tunable heating depending on the jar/bead compositions and size √ Adaptable to non-thermally conducting jars and to a large variety of readily-available jar/bead materials √ Potentially adaptable to *operando* analysis through other coil designs √ Potentially adaptable to other lab mills through other coil designs
Drawbacks	χ Heating of external walls of the jar only		χ Heating of external walls only (through air) χ Potentially inhomogeneous heating (heat-gun) χ Not adapted for Raman/XRD *operando* analyses		χ Potentially altered reactivity of reagents sensitive to magnetic fields, when using PMMA jars

mechanochemical reactions.[18] From a more general perspective, in order to broaden the scope of reactions accessible by mechanochemistry and to tune the product selectivity, various approaches have been proposed by different research groups to enable heating the reaction medium throughout the mechanochemical syntheses (see Table 1 and S5, ESI†).[10,15,17,19–32] Among these, one can mention (i) the use of a temperature-controllable heat-gun pointing towards a stainless steel milling jar, with the internal temperature of the milling system reaching up to ≈120 °C,[10] (ii) the design of special milling jars with a double envelope, in which boiling water is circulating at 96 °C,[23] and (iii) the wrapping of the milling jar by an aluminum sleeve, which is then heated using a proportional-integral-derivative (PID) thermal controller and can enable the external jar of the reactor to reach ≈250 °C for 1 hour.[17] From a synthetic perspective, such devices have shown to be very valuable not only to accelerate reaction kinetics or help overcome thermal activation barriers,[17] but also to help further

decipher the relative contributions of mechanochemical *vs.* thermal activations on the course of chemical reactions,[14,15] and to reduce the overall energy consumption during ball-milling reactions (by drastically reducing reaction times).[17]

Among the various heating systems proposed to date for ball-milling, most rely on heating the walls of a stainless steel (ss) reactor (Table 1). While some approaches can be very easily adapted to standard commercial ball-milling machines and jars (*e.g.* when using a heat-gun), they offer only little control over the rate of the heating.[10,27] *A contrario*, other approaches enable a more precise control over the temperature, but require PID-controlled heating systems for the reactors.[17,27] Moreover, it is important to highlight that in the majority of cases, the reported set-ups did not allow to follow the evolution of the heated reaction medium using *in situ* and/or *operando* analyses, such as Raman spectroscopy or X-ray diffraction, due to the nature of the reactors used (with opaque ss walls). Noticeable exceptions include the work by Užarević and co-workers, who designed a specific reactor with an included sapphire window to monitor ball-milling reactions under heat-treatment using Raman spectroscopy,[17] and the recent investigations by Michalchuck and co-workers.[29]

In this general context, because of the attractive prospect of being able to combine heating and milling (Table S5, ESI†), it appeared to us as an important goal to be able to propose alternative heating approaches, which would (i) be directly adaptable to standard commercially available ball-milling machines, without requiring a re-design of the milling jars (especially because synthesis outcomes can be modified when varying the geometry or composition of the milling jar and beads),[33,34] (ii) offer the possibility to perform the heating when using reactors transparent to X-ray or Raman-laser beams (*e.g.* made of PMMA or polycarbonate) in order to be able to carry out *in situ* and/or *operando* analyses of the media during the heating, and thereby follow the course of the reactions. Such requirements made us take interest in induction heating, which uses the Joule effect produced by Eddy currents generated in a conductor material when it is submitted to an alternating magnetic field. If this material presents also magnetic properties, then a new source of heat generation power occurs, called the hysteresis loss power phenomenon. Indeed, the work produced by the magnetic forces inside the material coming from the presence of an external alternating magnetic field is converted into heat. Thus, because in the vast majority of mechanochemical reactions, either the jar or the beads are made of stainless steel, it is in principle possible to easily heat these through application of an alternating magnetic field. Although induction heating is very commonly used, not only for research developments but also in a variety of industrial, domestic and medical applications, it has, to the best of our knowledge, only been recently proposed as a method to heat a continuous-flow bead mill,[31] but not yet for heating standard commercial ball-milling equipment.

The purpose of this manuscript is to perform a proof-of-concept study, to show how induction provides an attractive alternative for heating reaction media during ball-milling, when working under *standard* batch conditions, a method which will hereafter be named ''i-BM'' (standing for ''induction-heating ball-milling''). First, we will show how it can be directly adapted to available milling machines and reactors, and can be used to *selectively* heat either the walls of the reactor or the beads. Then, using the combination of several induction-heating experiments and a modeling of the physics of the system (including through numerical simulations), explanations to the changes in temperature of the jar and beads are provided. Lastly, examples of applications of this technique to ball-milling reactions will be presented, highlighting how it can be used to alter the physico-chemical properties of a milling medium (*e.g.* rheology, texture...), and/or how it can enable to prepare compounds which are inaccessible under standard ball-milling reactions (*i.e.* in absence of heating).

Results

Presentation of the experimental set-up for i-BM

Among the different mixer mills which have been used so far, the geometry of the P23 vertical mixer mill by Fritsch was found to be very well suited for testing the feasibility and versatility of induction heating. Indeed, as shown in Fig. 1, it allows the milling jar to be directly positioned at the center of a coil, without requiring any instrumental modification or adaptation. Here, the coil design was chosen such that it could receive currents of 320 A oscillating at a frequency which can be tuned between 100 and 350 kHz, while being cooled from the inside with circulating water. These oscillating currents generate an oscillating magnetic field at the same frequency, with typical field-lines as represented in Fig. 1b. By positioning a material which is sensitive to oscillating magnetic fields at the center of the coil, heating can occur through the heat power produced by the generation of Eddy currents (for conducting materials), and also by the hysteresis loss power phenomenon (for magnetic materials).

The induction-heating set-up shown in Fig. 1 appeared to us as highly attractive for testing different milling and heating conditions. In terms of milling, it enables the use of different types of milling jars, including commercial ss jars (which are the most commonly employed in ball-milling reactions), and plastic ones made of PMMA or polycarbonate (like the custom-made ones developed by the group of Prof. Franziska Emmerling,[14,46,47] which are widely used for Raman and X-ray *operando* analyses of ball-milling reactions). Moreover, in terms of heating, the system is very versatile, because the heating rate and maximum temperature achieved can be easily varied for a given coil geometry, by changing the intensity or frequency of the oscillating field. Therefore, in the prospect of performing i-BM reactions, these different aspects were investigated in more depth, using a combined experimental/modeling approach, as detailed below.

Different heating options, depending on the jar and beads

Two different {jar/bead} configurations were considered in view of performing i-BM reactions: a ss jar and ss beads on one

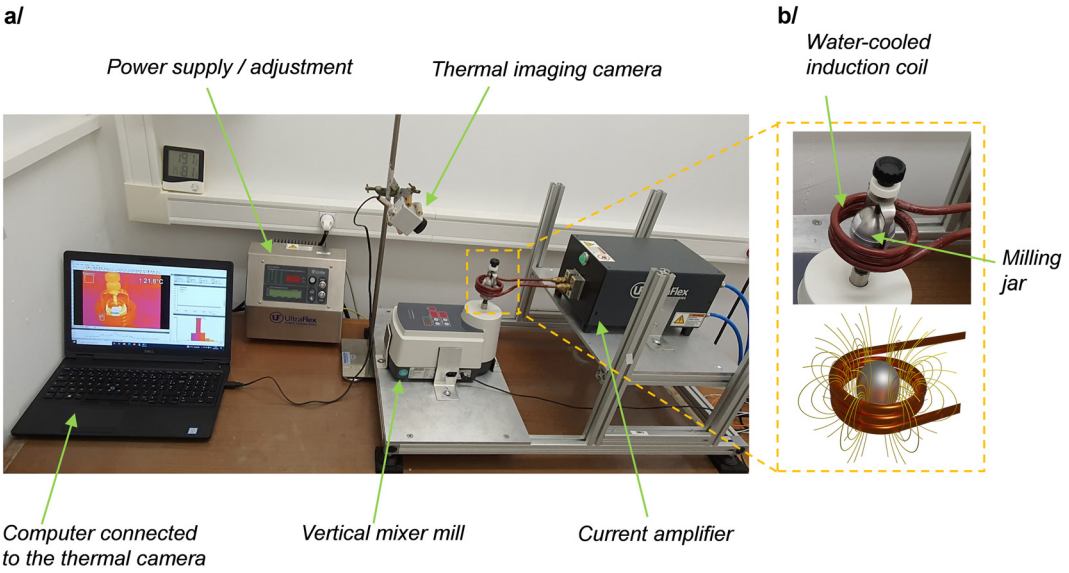

Fig. 1 (a) Representation of the experimental set-up used for induction heating during ball-milling (i-BM). (b) Zoom onto the milling jar and induction coil (top), and schematic representation of the magnetic field lines when current is circulating in the coil (bottom). Additional pictures and views of the instrumental set-up are provided in ESI† (Fig. S1).

hand, and a PMMA jar along with ss beads on the other. Initial simulations of the induction-heating under the influence of an oscillating magnetic field were carried out for both systems using the COMSOL software.[48] The experimental geometry of the jar/bead systems was simplified, by using a 2D model with a rotational symmetry (to generate a 3D model more straightforward to use in the subsequent calculations), while keeping the relative sizes of the jar and bead consistent with those used in our experiments. Moreover, a single bead was virtually positioned at the center of the jar (with no contact between the two), and both the jar and bead were kept static during the course of simulations. The latter point was found to be reasonable as a first approximation, based on complementary experiments (see Fig. S3, ESI†). The magnetic field generated was then calculated from the Maxwell equations, using experimental parameters for the current of coils, *i.e.* an alternating current amplitude between 0 and 320 A at a frequency of 161 kHz. In parallel of Maxwell equations, the heat equation was used to calculate the heat generation and propagation, and the Navier–Stokes equation was used to calculate the laminar flux (term of convection in the heat equation) of the air. For all these calculations, relevant parameters for the relative permeability, electric conductivity, heat capacity, density and thermal conductivity of ss and PMMA were used (see Table S2, ESI,† for further details).

Both jar/bead configurations led to very distinct outcomes regarding the magnetic field at the center of the coil (Fig. 2). On one hand, for the {ss jar/ss bead} system, the magnetic field lines enable to heat the jar's walls. Yet, these magnetic field lines are also screened by the walls (shielding), preventing them from penetrating inside the jar and from directly heating the beads inside the jar (Fig. 2a). This implies that only the outer shell of the jar can heat up upon application of an oscillating magnetic field, and that the bead positioned at the center of the milling jar remains essentially unaffected. On the other hand, for the {PMMA jar/ss bead} system, the magnetic field lines penetrate to the center of the PMMA jar, enabling the heating of the ss bead inside the jar (Fig. 2b). Concomitantly, only minimal heating of the jar occurs in these conditions, as expected from the PMMA material properties.

A series of experiments were subsequently carried out to study both of these configurations, and to confront results to simulations. First, regarding the {ss jar/ss bead} system, the bead was positioned at the center of the jar on a Teflon mat (to avoid direct contact with the jar walls). The jar was closed, and induction heating was applied while keeping the system static throughout the heating. The induction heating parameters were set such as to reach a final temperature $\approx$80 °C at the surface of the jar, and the total heating time was 2 minutes. The variation in the jar's temperature during the heating was monitored using a thermal camera (as detailed in ESI†), showing that the 80 °C target could be reached in less than 1 minute, and stayed stable afterwards. The temperature of the bead, on the other hand, could only be measured at the end of the 2 min heating, when opening the jar. As shown in Fig. 2a, it was observed that the ss bead temperature was indeed much lower than that of the external walls of the jar (by $\approx$40 °C in our experiments), as expected from simulations.

Concerning the {PMMA jar/ss bead} system, a similar experiment was performed, in which the ss bead was positioned at the center of the PMMA jar, which was closed and subjected to induction heating for a total time of 2 minutes, in "static" mode. As shown in Fig. 2b, at the end of the heating period, the jar's surface was mainly unchanged while the temperature of the bead (as estimated by opening the jar after the 2 minutes of heating) was $\approx$88 °C. This is thus also in line with the predictions made by simulations. To the best of our knowledge,

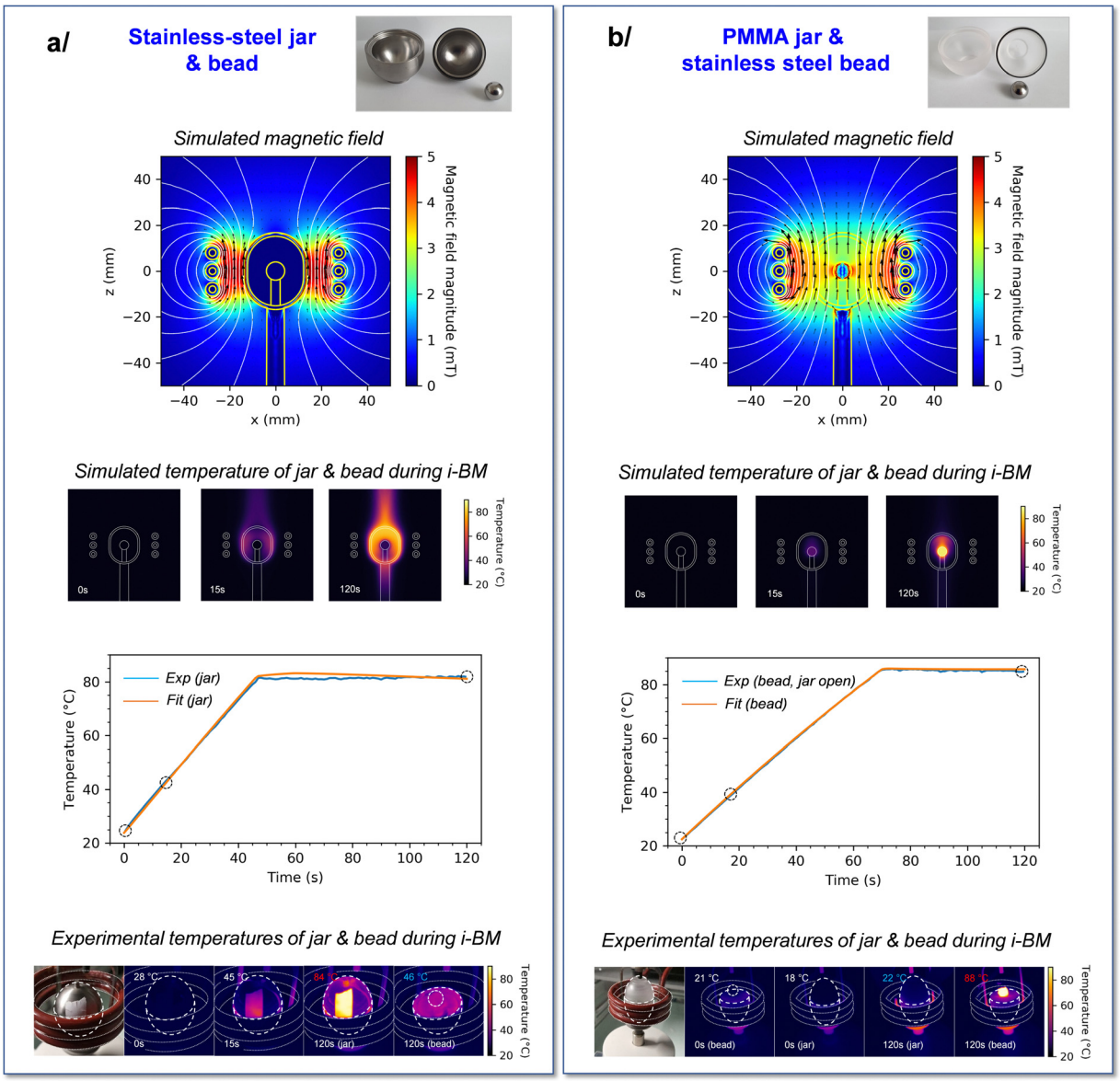

Fig. 2 Simulations and experiments performed on the two systems used for induction heating during ball-milling (i-BM): (a) {ss jar/ss bead} and (b) {PMMA jar/ss bead}. The experimental and simulation parameters used are provided in ESI† (Tables S1 and S2). Top: Simulated magnetic field lines; middle: simulations of the changes in temperature during i-BM at different time points, and graphical comparison of experimental and fitted temperatures of jar (left) and bead (right) during i-BM. Bottom: Photos and thermal images during i-BM, at the time-points indicated by circles on the graphs above, showing that after 120 s of i-BM, the temperature of the beads is moderate in (a) (*i.e.* lower than the temperature of the jar), but high in (b) (*i.e.* much higher than that of the jar). To enable temperature measurements on stainless steel using the IR-thermal imaging camera, a sticker was added on the jar (or bead), as discussed in ESI† (Fig. S2 and S6). The IR-thermal imaging camera was left running throughout the milling, including while opening the jar, to capture the temperature of the bead just at the end of the i-BM heating cycle.

it is the first time that such heating "directly from the inside" of the milling jar is proposed for mixer mills.

Importantly, for both the {ss jar/ss bead} and {PMMA jar/ss bead} systems, it is interesting to note that it was possible to set the induction heating parameters in a way that the temperature of the ss bead (or jar) remains relatively constant (±1 °C) when it reaches the plateau at ≈80 °C (see Table S1, ESI†). Moreover, using the experimental induction heating parameters, it was possible to model accurately the heating rate of the jar (in the former case) and bead (in the latter case), as well as the plateaus. This is illustrated at the bottom of Fig. 2a and b, where the discrepancy between experimental points (in blue) and simulated data (in orange) is very small. Examples of the repetition of a given heating condition for the {ss jar/ss bead} system are reported in ESI† (Fig. S4).

To go one step further, additional experiments were performed, showing that it is possible to stabilize the temperature of both types of configurations at lower values (*e.g.* ≈40 and 60 °C, Fig. 3a and c). Again, experimental data could be satisfactorily fitted using simulations. No attempt to reach

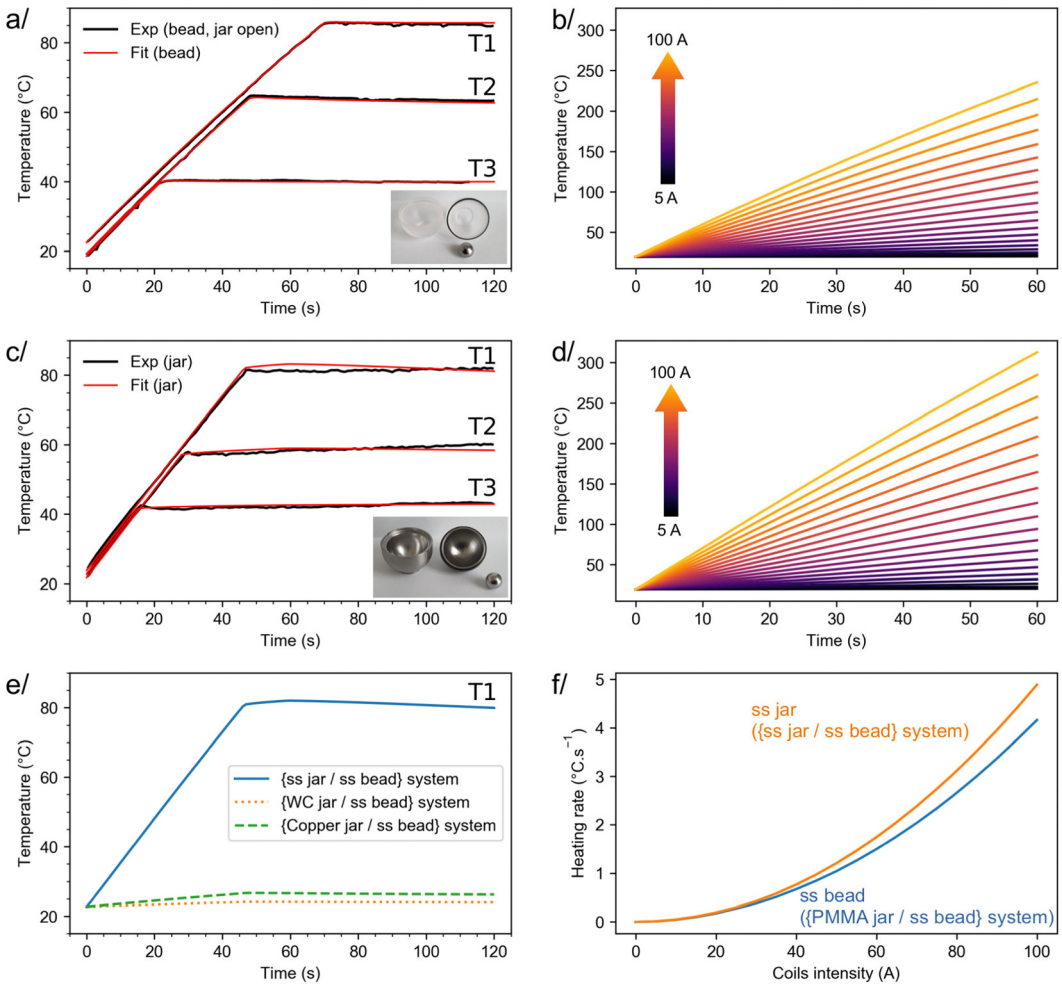

Fig. 3 On the left, experiments and fits performed on the {PMMA jar/ss bead} (a) and {ss jar/ss bead} (c) systems used for induction heating during ball-milling, showing that the temperature of the jar or bead can be stabilized at different values (noted here *T1*, *T2* and *T3*), depending on the i-BM parameters. On the right, simulations performed on the {PMMA jar/ss bead} (b) and {ss jar/ss bead} (d) systems, showing the influence of the coils' current on the maximum temperature achieved, and on the heating rate. (e) Simulations with the same condition as the {ss jar/ss bead} system stabilized at the *T1* temperature, when other jar materials are used. (f) Initial heating rate (at t = 0 s) as a function of the intensity in the coils, for the {ss jar/ss bead} and {PMMA jar/ss bead} systems. All parameters used in simulations are given in ESI,† in Tables S1 (current as a function of the time) and S2 (parameters related to the materials' properties).

higher temperatures *experimentally* was made at this stage, due to the current design of the milling equipment which involves standard rubber O-rings and joints. Nevertheless, because the simulations performed could convincingly reproduce the experimental curves at 40, 60 and 80 °C (see red *vs.* black curves in Fig. 3a and c), further simulations were then performed (i) to evaluate the influence of the induction heating parameters on the heating rate (dT/dt) and the maximum temperature reachable, and (ii) to study the potential effect of other parameters on the performance of this heating/milling system (*e.g.* composition of the beads).

As shown in Fig. 3d, simulations predict that in the case of the {ss jar/ss bead} system, by varying the coil current (I) up to 100 A, temperatures as high as ≈300 °C can potentially be easily reached by induction heating after just 1 minute. Along the same line, these simulations show how the heating rate can be tuned by changing the current in the coils (see Fig. 3f), allowing a temperature ≈80 °C to be accessed in just 15 s. Similar trends can be derived for the {PMMA jar/ss bead} system, the difference being that it is no longer the jar which gets heated but the bead itself (see Fig. 3b and f). The small discrepancies between the heating rates of both systems, as illustrated in Fig. 3f, are mainly due to the differences in size and shape of the heated ss objects (*i.e.* jar *vs.* bead). Thus, i-BM appears as an attractive method to finely control the heating conditions during BM, and both mathematical functions relating the heating rate and maximum temperature as a function of I (showing a I^2 dependency, as explained in ESI,† Section II-c) can be used as a guideline for setting up future experiments and achieving a specific temperature.

Given that in the literature, several examples highlight the advantages of being able to vary the composition of milling jars and beads in mechanochemistry,[33,34,49–51] additional tests were also carried out to determine how i-BM can be adapted to other

jars, such as those made of tungsten carbide (WC) and copper, or to other beads, such as the commercially available ones made of a ss core coated by a PTFE layer (noted hereafter as ss@PTFE), which are interesting to use for reactions involving reagents that are incompatible with metallic milling jars/beads. First, using simulations (Fig. 3e), it was found that for the same induction current (maximum of 50 A), the heat produced by a material with intrinsic magnetic properties like ss is unbeatable, in comparison to non-magnetic materials like copper and tungsten carbide: a temperature increase ΔT of $\approx$60 °C and $\approx$4 °C was calculated for ss and copper, respectively. The heating current used in i-BM would need to be further increased to achieve a more pronounced heating of Cu and WC jars. Second, regarding the ss@PTFE beads, complementary experiments and simulations were performed (Fig. S5, ESI†), showing that when covered by a PTFE coating, the heating produced by a ss bead is still significant. Indeed, under the heating conditions we tested (*i.e.* with a maximum induction current of 50 A), a stable temperature $\approx$40 °C could be reached for the ss@PTFE bead. Based on simulations like the one reported in Fig. 3f, an even more pronounced heating of the ss core (and thus of the PTFE shell) should be achievable by further increasing the current in the coil. Overall, these additional experiments and simulations point to how i-BM can be used with different types of milling jars and beads, making it adaptable to a wide diversity of BM reactions.

Lastly, because other geometries of milling jars are also commonly employed in mechanochemistry, complementary simulations were also performed, to evaluate how these may affect the outcome of i-BM reactions. As shown in Fig. S8 in ESI,† when using cylindrical-shaped jars, similar outcomes can be expected as for the more spherical reactors. Indeed, in the case of ss jars, a screening effect will occur, which leads to a confinement of the magnetic field at the metal's surface. The heat generation is then located on the surface of the jar, and the heat dissipation will depend on the surface-to-volume ratio of the jar. In other words, the shape of the jar will affect the temperature evolution during the i-BM process. In the case of PMMA jars, however, because the material is an insulator, there is no screening effect, and the jar is "transparent" to magnetic fields (whatever its geometry). Overall, such simulations can provide preliminary guidelines as to how to further adapt and use i-BM in a wide diversity of reactions. Last but not least, it is interesting to note that, due to its simple composition and geometry (copper pipes), the coil design is also highly adjustable to different jar geometries and different milling configurations, and can provide additional options to further tune the i-BM process, so that it can be adapted to other milling equipment and set-ups (including for *operando* analyses).

Having demonstrated the versatility of i-BM for heating different reaction media in mechanochemistry, its interest for various specific applications was then looked into, when using either {ss jar/ss bead}, or {PMMA jar/ss bead} systems, as described in the next section.

Applications of i-BM to the study of different reaction systems

Studying mechanisms in mechanochemical reactions. As mentioned in the introduction, one of the major goals today in the field of mechanochemistry is to be able to understand the details of reaction mechanisms, including deciphering the relative contributions of milling and heating during reactions. This is particularly important when it comes to synthesizing compounds and materials of high added-value using mechanochemistry, such as isotopically enriched ones, as it may help reach higher purity phases with higher enrichment levels. Thus, we decided to see how using i-BM, further improvements in oxygen-17 isotopic labeling schemes could be achieved (^{17}O being a highly valuable isotope for NMR spectroscopy, which suffers from a very low natural abundance of only 0.04%). Two examples are provided below, in the context of the oxygen-isotopic labeling of silica on one hand, and of fatty acids on the other.

In a recent work by Chen *et al.*, it had been shown that ^{17}O-enriched silica can be prepared using mechanochemistry,[52] starting from fumed silica (Aerosil 200, a porous form of silica, made of aggregated nanoparticles), and performing the milling for 15 minutes in a vertical mixer mill in presence of stoichiometric amounts of ^{17}O enriched water. Although the ^{17}O-labeling was successful, the enrichment level achieved was only $\approx$5%, which is beneath the maximum value potentially accessible given the amount of labeled water engaged. To further increase the amount of ^{17}O-enriched siloxanes, several options can be considered, like (i) increasing the amount of enriched water used in the reaction (which is not an attractive alternative, considering the high cost of ^{17}O-enriched water), (ii) further increasing milling time (which may imply a more significant contamination of the powder by the wear of the ss jar),[53] or (iii) heating the medium during the milling in order to accelerate the kinetics of the reaction. Given that the vertical mixer mill which had been used by Chen *et al.* is precisely the one adapted to i-BM heating, the latter option was looked into here.

Fumed silica was milled in presence of ^{17}O-enriched water, at room temperature (*i.e.* without heating) or using i-BM (*i.e.* heating at $\approx$65 °C) for 5 and 15 minutes. The ^{17}O solid state NMR spectra of the different phases were then recorded under identical measurement conditions, focusing in all cases on the signature of ^{17}O-labeled siloxane bridges (Fig. 4a). The amount of enriched siloxanes was found to increase between 5 and 15 minutes of milling, in agreement with previous observations.[52] However, no further enrichment was observed when using i-BM. This implies that the kinetics of isotopic labeling of siloxanes are mainly limited by the actual milling process (rather than by the need to cross an activation barrier through heat-treatment), and that it is more the disruptions caused at the surface of the particles during the milling which enable creation of reactive surface sites, for the siloxane enrichment to take place. This conclusion is further supported by the fact that (i) only small changes in the specific surface area and distribution in volume of the pore sizes occur when adding heating during the milling (Fig. 4b), and (ii) a lower level of enrichment occurs when milling at room temperature a crystalline form of silica (quartz microparticles) compared to aerosil.[52] Such insight into the enrichment mechanism of silica

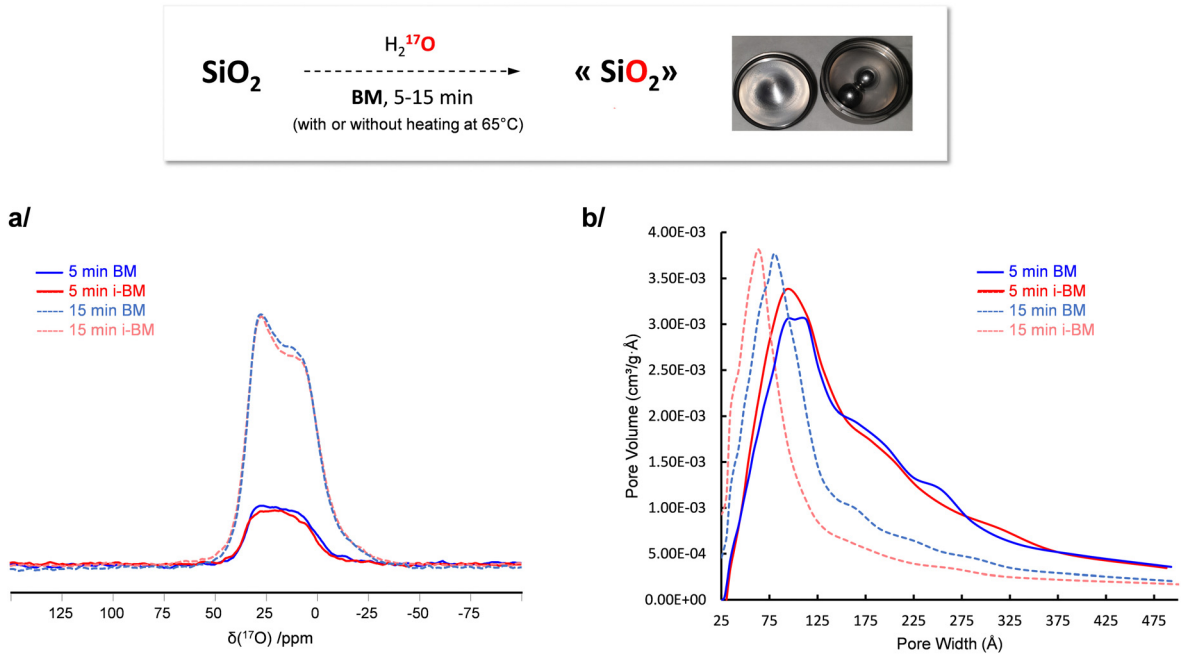

Fig. 4 Influence of i-BM on the isotopic labeling of fumed silica. (a) ^{17}O MAS NMR spectra, and (b) comparison of the pore size distribution (as determined from N_2 adsorption measurements, using the Barrett, Joyner et Halenda – BJH – model, as in our previous study on the ^{17}O-labeling of silica),[52] for phases prepared after 5 and 15 minutes milling, with (red) or without (blue) i-BM.

is particularly valuable in view of further optimizations of the labeling: it suggests that it is more by using different silica precursors (with different particle size or surface area), or different milling configurations (*e.g.* different type of mixer mill, or change in material, size and number of beads used) that a more extensive enrichment may be achieved.

Still in the context of ^{17}O isotopic labeling, an extensive study of the enrichment of fatty acids using mechanochemistry was performed recently by Špačková *et al.*[16] For reactions in which the labeling step consisted in hydrolyzing a fatty acid which had been activated using CDI (1,1′-carbonyldiimidazole), a correlation had been found between the duration of the hydrolysis and the chain length of the fatty acid, those with the highest melting points requiring much longer milling times for the hydrolysis. For example, the hydrolysis time increased from 1 to 3 h when switching from lauric acid (C12) to palmitic acid (C16). For even longer chains, like stearic acid (C18), complete hydrolysis could only be reached after 3 h of milling upon addition of an additional base (K_2CO_3). It was thus hypothesized that by using i-BM, a reduction in the hydrolysis time should be achieved, and that it may become possible to enrich very long chain fatty acids (VLCFA, which have at least 22 carbon atoms).

A series of experiments were first carried out on palmitic acid. For this compound, the melting of the activated intermediate mixture had been measured to start around 73 °C. The hydrolysis was thus performed with and without i-BM, while setting the heating temperature at ≈70 °C. As shown using IR spectroscopy, after only 5 minutes of milling at 30 Hz, the C=O stretching band characteristic of the activated form disappeared, showing that the hydrolysis is complete (Fig. 5a, green *vs.* orange spectra, and Fig. S9 and S12 in ESI†). In absence of heating, no such observation was made, even after 1 hour of milling (Fig. 5a, blue spectrum). Similarly, in the case of stearic acid, the hydrolysis time could be reduced to less than 15 minutes when performing i-BM at a heating temperature close to the melting point of the activated mixture, without needing to use an additional base, which is a significant improvement to the previously established protocol (Fig. 5b and Fig. S10, S13 in ESI†). These observations confirm that, as hypothesized in our earlier work,[16] it is indeed the change in physical state of the reactive species in the heated BM medium which enables the hydrolysis to occur. Based on these results, for the first time, the oxygen isotopic labeling of a VLCFA (behenic acid, C22) could be achieved in only 15 minutes using i-BM, while heating at 90 °C (Fig. 5c and Fig. S11 in ESI†). Such experiments clearly show how i-BM can be used to improve the efficiency and substrate-scope of ball-milling reactions, by altering the physico-chemical properties of the reaction medium (in this case to reach the melting point), and favoring the better mixing of reagents.

Changing the physico-chemical properties of milling media. One phenomenon which has been reported to occur during some ball-milling reactions is the so-called "snowball" effect. It corresponds to a physical change in the medium, during which the reagents/products progressively cover the beads during the milling process, until a relatively thick layer remains at the surface of the beads. To the best of our knowledge, this effect was initially reported by Boldyreva, during the grinding of oxalic acid dihydrate and glycine: in this case the formation

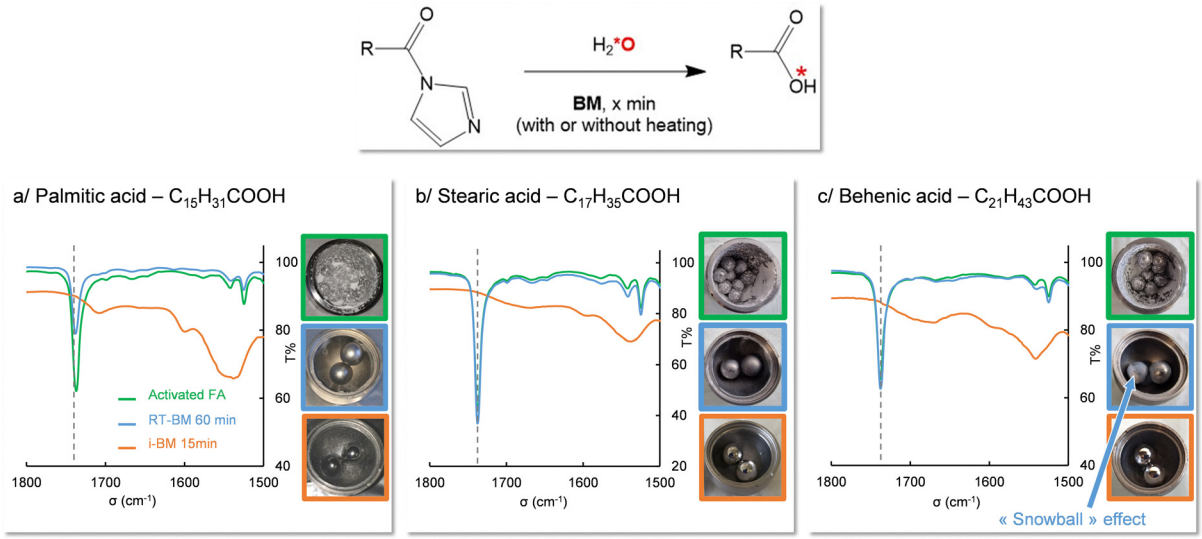

Fig. 5 Influence of i-BM on the isotopic labeling of fatty acids, as demonstrated using IR spectroscopy, for (a) palmitic acid ($T_{melt} \approx 73$ °C; $T_{i\text{-}BM} = 70$ °C), (b) stearic acid ($T_{melt} \approx 78$ °C; $T_{i\text{-}BM} = 85$ °C), and (c) behenic acid ($T_{melt} \approx 90$ °C; $T_{i\text{-}BM} = 90$ °C). IR spectra of the activated FA (green), BM-hydrolysis test at room-temperature (blue, after 60 min milling) and under i-BM conditions (orange, after 15 min milling) are shown, with the dashed vertical line pointing to the C=O stretching frequency of the activated FA. Hydrolysis reactions were optimized using non-labeled or ^{18}O-enriched water (to check the feasibility of i-BM reactions), prior to working with ^{17}O-enriched water, in line with our previous work (which had shown that no isotopic effect on the hydrolysis rate would occur upon switching to ^{17}O/^{18}O-enriched water). Characterizations by mass-spectrometry of oxygen-labeled compounds are provided in ESI,† together with ^{1}H solution NMR analyses confirming the purity of the isolated products (Fig. S9–S13 in ESI†).

of the snowball was explained by a caking effect, induced by the release of a stoichiometric amount of liquid (coming from the water molecules of the oxalic acid dihydrate).[54] Similarly, Hutchings *et al.*, as well as Carta *et al.*, noted the formation of a robust coating around the milling beads during the mechanochemical Knoevenagel condensation of barbituric acid and vanillin.[55,56] Moreover, Andersen *et al.* used Al_2O_3 as an additive during a proline-catalysed aldol reaction performed by mechanochemistry, and observed the formation of a snowball.[57] More recently, Leroy *et al.* reported the transient formation of a snowball upon the progressive hydrolysis of fumed silica under mechanochemical conditions.[58]

The formation of snowballs can be seen as potentially problematic to ball-milling reactions, by preventing a proper mixing of the different reagents, potentially leading to inhomogeneous mixtures. As a matter of fact, in the case of the hydrolysis test on activated behenic acid (Fig. 5c), a "snowball" was observed after one hour of milling at room temperature,

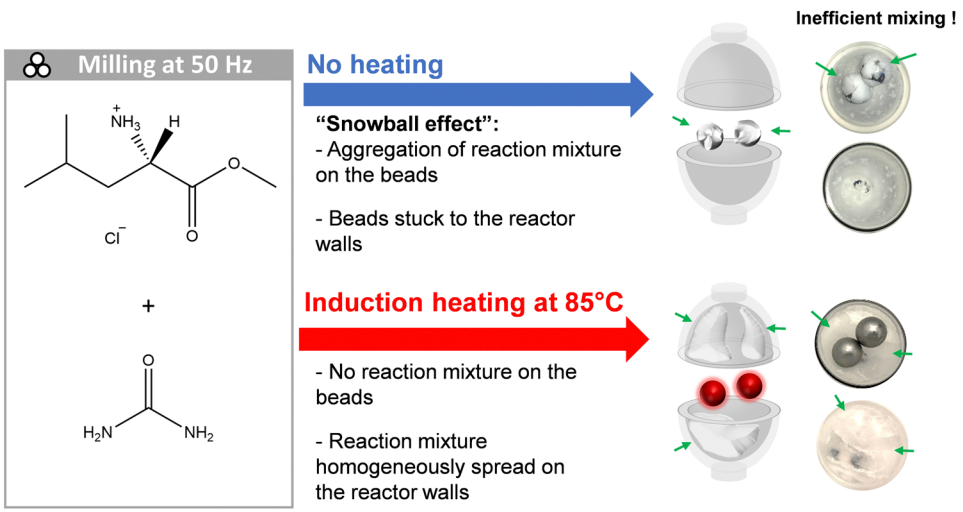

Fig. 6 Comparative scheme of the cogrinding of urea (melting point = 133–135 °C) with L-leucine methyl ester hydrochloride (melting point = 151–153 °C), leading to the formation of a new cocrystal (melting point = 87–92 °C). On top, in absence of i-BM, the snowball phenomenon occurs after 4–5 min of milling at 50 Hz. On the bottom, when using i-BM to quickly heat the two ss beads through the PMMA jar up to 85 °C in a few seconds, the formation of the snowball is prevented. A video showing the formation of the "snowball", and its subsequent disappearance under i-BM is provided in ESI.†

which could explain (at least in part), the lack of efficient mixing between reagents, and the absence of hydrolysis of the activated intermediate according to IR analyses. Hence, being able to prevent their formation by altering the physico-chemical properties of the ball-milling medium through temperature treatment is an attractive feature.

In the course of a study involving the cogrinding urea with L-leucine methyl ester hydrochloride using a vertical P23 mixer-mill (see Fig. 6), we noticed a drastic change of physical aspect of the reagents, switching from free-flowing powders to a sticky rubber-like material, and progressively forming an envelope around the beads (snowball). Although we were able to form a new product (see Fig. S14 in ESI†), in some of the trials, the stickiness of the materials covering the balls severely hampered the milling process, up to a point that the motions of the beads were sometimes completely stopped, as they stayed ''stuck'' on the reactor's walls. In such conditions, the conversion can be potentially incomplete, and/or can vary in different parts of the milling medium. Here, by using i-BM (heating of the stainless steel beads up to 85 °C during the cogrinding), we were able to avoid the formation of a snowball (see Fig. 6, and video in ESI†). Thus, this example illustrates the versatility offered by the i-BM method, not only to help achieve new chemical reactions, but also as a straightforward approach to modify the texture of reagents and the physical properties of reaction media.

Conclusion & perspectives

To conclude, in the present work, we have brought forward some of the numerous possibilities offered by induction heating in ball-milling, using a combined experimental/simulation approach. The instrumental set-up we have proposed is attractive, because (i) it is directly adaptable to commercially-available milling equipment and to a wide variety of milling jars and beads, (ii) it can enable a very fast heating of milling media (by controlling the induction-current parameters), and (iii) it can be used to heat either the walls of the milling jars or the beads themselves, depending on the choice of the materials which compose them. Importantly, our methodology allows the heating of a milling medium ''from the inside'' (when using a PMMA jar and ss beads, for example), which is an original feature compared to previously reported heating systems (Table 1). First examples of applications of this option are shown here in the study of snowball effects. On a broader perspective, such a feature also opens the way to ''real-time'' studies of BM reactions under heating conditions using standard techniques like Raman spectroscopy, which require ''transparent'' jars (*e.g.* made of PMMA or polycarbonate), and which are still only occasionally studied in mechanochemistry combinations with heating. Thus, such *operando* analyses coupled to i-BM should favour a better optimisation of heating/milling conditions, and participate to the discovery of reaction intermediates, new reactivities and new selectivities in the near future.

Using numerical simulations, it was shown how i-BM enables to finely tune the heating conditions (*e.g.* heating rate and maximum temperature reached), by playing with the nature of the milling system and/or the induction heating currents used. While simulations were mainly performed here to provide guidelines to evaluate the influence of different parameters under standard ''continuous heating'' conditions, they actually also provide additional interesting information. They suggest, for example, that reagents sensitive to magnetic fields should not behave much differently in i-BM compared to a-magnetic ones when using a {ss jars/ss beads} configuration because the magnetic field lines are expelled from the jar (Fig. 2a), while, *a contrario*, they could lead to different reactivity in the case of the {PMMA jar/ss beads} configuration, as they will be exposed to the field (Fig. 2b). On a longer perspective, using i-BM, it will also be possible to apply ''heating pulses'' to the milled medium, during which the temperature can periodically reach temperatures $\approx$100 °C in just a few seconds (when using a PMMA-jar/ss bead set-up for example). This is an original feature in comparison to other heating devices proposed thus far, which further broadens the scope of reaction conditions made available to chemists. Results along this line will be reported in due course.

Experimental details

Equipment for milling and induction heating

The majority of the mechanochemical syntheses were performed with a Fritsch Pulverisette-23 (P23) vertical mixer mill, using 10 mL inner-volume jars made of PMMA or stainless steel, with 10 mm diameter stainless steel beads. Induction heating ball-milling experiments (i-BM) were performed with this milling equipment. Temperature measurements were performed using an OPTRIS PI450i thermal imaging camera. Further details on the experimental set-up can be found in ESI† (Section I), including in Fig. S1 (ESI†). Information on the accuracy of temperature measurements is provided in pages S3 and S4 of the ESI,† and the reproducibility of the plateau temperature reached for different tests is shown in Fig. S4 (ESI†).

Computational modeling

All numerical simulations were carried out using the COMSOL software suite (version 6.0) with the AC/DC module.[48] The simulations were run on a Dell Precision 5820 workstation, consisting of an Intel Xeon W-2275 (14-core HT, 3.3 GHz, 4.8 GHz Turbo, 19.25 M cache, 165 W) processor and 64 Go of RAM; a typical simulation took less than 2 minutes. The optimization of the fit parameters was performed using a homemade Python script involving the mph and SciPy libraries.[59] Further details on the equations used for the fits, including the physical constants of the materials composing the jars and beads, are provided in ESI† (Section II).

Ball-milling syntheses

Reagent-grade precursors were used in all reactions, and the products formed were all characterized using standard analytical techniques (see ESI†).

The ^{17}O-labeling of silica under i-BM was performed by adapting our previously reported procedure (see ESI,† Section III-b).[52] The activation and hydrolysis of palmitic, stearic and behenic acids under i-BM was carried out by adapting previously used reaction conditions, as further detailed in ESI† (Section III-c).[16,60] A co-crystal between L-leucine methyl ester hydrochloride and urea was obtained by milling both reagents in stoichiometric conditions, as described in ESI† (Section III-d).

Author contributions

The study was conducted by DL and GF, in close interaction with all co-authors. NF, GF and DL worked on the design and optimization of the instrumental set-up for i-BM. NF, CL, CHC and DL performed the i-BM experiments. GF carried out the numerical simulations. NF, CL, CHC, TXM and DL interpreted the results of the syntheses and characterizations. All co-authors participated to the writing of the manuscript (including figures and table preparations).

Data availability

All data supporting the findings of this study are available within the article and supplementary information files, and also are available from the corresponding authors upon reasonable request.

Conflicts of interest

The authors declare no competing interests.

Acknowledgements

This project has received funding from the European Research Council (ERC) under the European Union's Horizon 2020 research and innovation program (Grant 772204; 2017 ERC-COG, MISOTOP project). We acknowledge Prof. Franziska Emmerling for providing the PMMA reactors used for some of the syntheses shown here.

References

1 R. T. O'Neill and R. Boulatov, The many flavours of mechanochemistry and its plausible conceptual underpinnings, *Nat. Rev. Chem.*, 2021, **5**, 148–167.
2 K. Kubota and H. Ito, Mechanochemical Cross-Coupling Reactions, *Trends Chem.*, 2020, **2**, 1066–1081.
3 T. Friščić, C. Mottillo and H. M. Titi, Mechanochemistry for Synthesis, *Angew. Chem., Int. Ed.*, 2020, **59**, 1018–1029.
4 K. J. Ardila-Fierro and J. G. Hernández, Sustainability Assessment of Mechanochemistry by Using the Twelve Principles of Green Chemistry, *ChemSusChem*, 2021, **14**, 2145–2162.
5 J. G. Hernández and C. Bolm, Altering Product Selectivity by Mechanochemistry, *J. Org. Chem.*, 2017, **82**, 4007–4019.
6 G. Ayoub, B. Karadeniz, A. J. Howarth, O. K. Farha, I. Đilović, L. S. Germann, R. E. Dinnebier, K. Užarević and T. Friščić, Rational Synthesis of Mixed-Metal Microporous Metal–Organic Frameworks with Controlled Composition Using Mechanochemistry, *Chem. Mater.*, 2019, **31**, 5494–5501.
7 A. Garci, K. J. Castor, J. Fakhoury, J.-L. Do, J. Di Trani, P. Chidchob, R. S. Stein, A. K. Mittermaier, T. Friščić and H. Sleiman, Efficient and Rapid Mechanochemical Assembly of Platinum(II) Squares for Guanine Quadruplex Targeting, *J. Am. Chem. Soc.*, 2017, **139**, 16913–16922.
8 P. F. M. de Oliveira, A. A. L. Michalchuk, A. G. Buzanich, R. Bienert, R. M. Torresi, P. H. C. Camargo and F. Emmerling, Tandem X-ray absorption spectroscopy and scattering for in situ time-resolved monitoring of gold nanoparticle mechanosynthesis, *Chem. Commun.*, 2020, **56**, 10329–10332.
9 J. A. Leitch, H. R. Smallman and D. L. Browne, Solvent-Minimized Synthesis of 4CzIPN and Related Organic Fluorophores via Ball Milling, *J. Org. Chem.*, 2021, **86**, 14095–14101.
10 T. Seo, N. Toyoshima, K. Kubota and H. Ito, Tackling Solubility Issues in Organic Synthesis: Solid-State Cross-Coupling of Insoluble Aryl Halides, *J. Am. Chem. Soc.*, 2021, **143**, 6165–6175.
11 C. Bolm and J. G. Hernández, From Synthesis of Amino Acids and Peptides to Enzymatic Catalysis: A Bottom-Up Approach in Mechanochemistry, *ChemSusChem*, 2018, **11**, 1410–1420.
12 C. Leroy, T.-X. Métro, I. Hung, Z. Gan, C. Gervais and D. Laurencin, From Operando Raman Mechanochemistry to ''NMR Crystallography'': Understanding the Structures and Interconversion of Zn-Terephthalate Networks Using Selective ^{17}O-Labeling, *Chem. Mater.*, 2022, **34**, 2292–2312.
13 K. Užarević, N. Ferdelji, T. Mrla, P. A. Julien, B. Halasz, T. Friščić and I. Halasz, Enthalpy *vs.* friction: heat flow modelling of unexpected temperature profiles in mechanochemistry of metal–organic frameworks, *Chem. Sci.*, 2018, **9**, 2525–2532.
14 H. Kulla, M. Wilke, F. Fischer, M. Röllig, C. Maierhofer and F. Emmerling, Warming up for mechanosynthesis – temperature development in ball mills during synthesis, *Chem. Commun.*, 2017, **53**, 1664–1667.
15 J. M. Andersen and J. Mack, Decoupling the Arrhenius equation via mechanochemistry, *Chem. Sci.*, 2017, **8**, 5447–5453.
16 J. Špačková, C. Fabra, G. Cazals, M. Hubert-Roux, I. Schmitz-Afonso, I. Goldberga, D. Berthomieu, A. Lebrun, T.-X. Métro and D. Laurencin, Cost-efficient and user-friendly ^{17}O/^{18}O labeling procedures of fatty acids using mechanochemistry, *Chem. Commun.*, 2021, **57**, 6812–6815.
17 N. Cindro, M. Tireli, B. Karadeniz, T. Mrla and K. Užarević, Investigations of Thermally Controlled Mechanochemical Milling Reactions, *ACS Sustainable Chem. Eng.*, 2019, **7**, 16301–16309.
18 K. Užarević, V. Štrukil, C. Mottillo, P. A. Julien, A. Puškarić, T. Friščić and I. Halasz, Exploring the Effect of Temperature

on a Mechanochemical Reaction by in Situ Synchrotron Powder X-ray Diffraction, *Cryst. Growth Des.*, 2016, **16**, 2342–2347.

19 J. M. Andersen and H. F. Starbuck, Rate and Yield Enhancements in Nucleophilic Aromatic Substitution Reactions via Mechanochemistry, *J. Org. Chem.*, 2021, **86**, 13983–13989.

20 J. Andersen, H. Starbuck, T. Current, S. Martin and J. Mack, Milligram-scale, temperature-controlled ball milling to provide an informed basis for scale-up to reactive extrusion, *Green Chem.*, 2021, **23**, 8501–8509.

21 S. Immohr, M. Felderhoff, C. Weidenthaler and F. Schüth, An Orders-of-Magnitude Increase in the Rate of the Solid-Catalyzed CO Oxidation by In Situ Ball Milling, *Angew. Chem., Int. Ed.*, 2013, **52**, 12688–12691.

22 G. Báti, D. Csókás, T. Yong, S. M. Tam, R. R. S. Shi, R. D. Webster, I. Pápai, F. García and M. C. Stuparu, Mechanochemical Synthesis of Corannulene-Based Curved Nanographenes, *Angew. Chem., Int. Ed.*, 2020, **59**, 21620–21626.

23 S. Mashkouri and M. Reza Naimi-Jamal, Mechanochemical Solvent-Free and Catalyst-Free One-Pot Synthesis of Pyrano[2,3-d]Pyrimidine-2,4(1*H*,3*H*)-Diones with Quantitative Yields, *Molecules*, 2009, **14**, 474–479.

24 G. Kaupp, Solid-state molecular syntheses: complete reactions without auxiliaries based on the new solid-state mechanism, *CrystEngComm*, 2003, **5**, 117.

25 **https://www.retsch.fr/fr/produits/broyer/broyeurs-a-billes/mm-500-control/**.

26 R. Takahashi, A. Hu, P. Gao, Y. Gao, Y. Pang, T. Seo, J. Jiang, S. Maeda, H. Takaya, K. Kubota and H. Ito, Mechanochemical synthesis of magnesium-based carbon nucleophiles in air and their use in organic synthesis, *Nat. Commun.*, 2021, **12**, 6691.

27 R. R. A. Bolt, S. E. Raby-Buck, K. Ingram, J. A. Leitch and D. L. Browne, Temperature-Controlled Mechanochemistry for the Nickel-Catalyzed Suzuki–Miyaura-Type Coupling of Aryl Sulfamates via Ball Milling and Twin-Screw Extrusion, *Angew. Chem., Int. Ed.*, 2022, e202210508.

28 V. Martinez, T. Stolar, B. Karadeniz, I. Brekalo and K. Užarević, Advancing mechanochemical synthesis by combining milling with different energy sources, *Nat. Rev. Chem.*, 2022, **7**, 51–65.

29 K. Linberg, B. Röder, D. Al-Sabbagh, F. Emmerling and A. A. L. Michalchuk, Controlling polymorphism in molecular cocrystals by variable temperature ball milling, *Faraday Discuss.*, 2023, **241**, 178–193.

30 I. Brekalo, V. Martinez, B. Karadeniz, P. Orešković, D. Drapanauskaite, H. Vriesema, R. Stenekes, M. Etter, I. Dejanović, J. Baltrusaitis and K. Užarević, Scale-Up of Agrochemical Urea-Gypsum Cocrystal Synthesis Using Thermally Controlled Mechanochemistry, *ACS Sustainable Chem. Eng.*, 2022, **10**, 6743–6754.

31 J. Thiel, F. Lacoste, V. Lair, S. Halloumi, I. Malpartida and B. Moevus, *Three-dimensional grinder, method for implementing same and uses thereof*. 2019, WO2019228983A1.

32 **https://impact-reactor.wab-group.com/**.

33 L. Catalano, L. S. Germann, P. A. Julien, M. Arhangelskis, I. Halasz, K. Užarević, M. Etter, R. E. Dinnebier, M. Ursini, M. Cametti, J. Martí-Rujas, T. Friščić, P. Metrangolo, G. Resnati and G. Terraneo, Open versus Interpenetrated: Switchable Supramolecular Trajectories in Mechanosynthesis of a Halogen-Bonded Borromean Network, *Chem*, 2021, **7**, 146–154.

34 A. A. L. Michalchuk, I. A. Tumanov and E. V. Boldyreva, Ball size or ball mass – what matters in organic mechanochemical synthesis?, *CrystEngComm*, 2019, **21**, 2174–2179.

35 G. Kaupp, How are Waste Entirely Avoided in Solid-State Productions?, *J. Chem. Eng. Process Technol.*, 2017, **08**, 1000335.

36 R. Schmidt, C. F. Burmeister, M. Baláž, A. Kwade and A. Stolle, Effect of Reaction Parameters on the Synthesis of 5-Arylidene Barbituric Acid Derivatives in Ball Mills, *Org. Process Res. Dev.*, 2015, **19**, 427–436.

37 G. Kaupp, M. R. Naimi-Jamal and V. Stepanenko, Waste-Free and Facile Solid-State Protection of Diamines, Anthranilic Acid, Diols, and Polyols with Phenylboronic Acid, *Chem. – Eur. J.*, 2003, **9**, 4156–4161.

38 J. Andersen and J. Mack, Insights into Mechanochemical Reactions at Targetable and Stable, Sub-ambient Temperatures, *Angew. Chem., Int. Ed.*, 2018, **57**, 13062–13065.

39 P. Gao, J. Jiang, S. Maeda, K. Kubota and H. Ito, Mechanochemically Generated Calcium-Based Heavy Grignard Reagents and Their Application to Carbon–Carbon Bond-Forming Reactions, *Angew. Chem., Int. Ed.*, 2022, e202207118.

40 R. Takahashi, T. Seo, K. Kubota and H. Ito, Palladium-Catalyzed Solid-State Polyfluoroarylation of Aryl Halides Using Mechanochemistry, *ACS Catal.*, 2021, **11**, 14803–14810.

41 Y. Gao, C. Feng, T. Seo, K. Kubota and H. Ito, Efficient access to materials-oriented aromatic alkynes via the mechanochemical Sonogashira coupling of solid aryl halides with large polycyclic conjugated systems, *Chem. Sci.*, 2022, **13**, 430–438.

42 K. Kubota, T. Endo, M. Uesugi, Y. Hayashi and H. Ito, Solid-State C−N Cross-Coupling Reactions with Carbazoles as Nitrogen Nucleophiles Using Mechanochemistry, *ChemSusChem*, 2022, **15**, e202102132.

43 J. Zhang, P. Zhang, Y. Ma and M. Szostak, Mechanochemical Synthesis of Ketones via Chemoselective Suzuki-Miyaura Cross-Coupling of Acyl Chlorides, *Org. Lett.*, 2022, **24**, 2338–2343.

44 K. L. Chagoya, D. J. Nash, T. Jiang, D. Le, S. Alayoglu, K. B. Idrees, X. Zhang, O. K. Farha, J. K. Harper, T. S. Rahman and R. G. Blair, Mechanically Enhanced Catalytic Reduction of Carbon Dioxide over Defect Hexagonal Boron Nitride, *ACS Sustainable Chem. Eng.*, 2021, **9**, 2447–2455.

45 R. Eckert, M. Felderhoff and F. Schüth, Preferential Carbon Monoxide Oxidation over Copper-Based Catalysts under In Situ Ball Milling, *Angew. Chem., Int. Ed.*, 2017, **56**, 2445–2448.

46 H. Kulla, S. Haferkamp, I. Akhmetova, M. Röllig, C. Maierhofer, K. Rademann and F. Emmerling, In Situ Investigations of Mechanochemical One-Pot Syntheses, *Angew. Chem., Int. Ed.*, 2018, **57**, 5930–5933.

47 L. Batzdorf, F. Fischer, M. Wilke, K.-J. Wenzel and F. Emmerling, Direct In Situ Investigation of Milling Reactions Using Combined X-ray Diffraction and Raman Spectroscopy, *Angew. Chem., Int. Ed.*, 2015, **54**, 1799–1802.

48 COMSOL AB, **www.comsol.com**.

49 D. A. Fulmer, W. C. Shearouse, S. T. Medonza and J. Mack, Solvent-free Sonogashira coupling reaction via high speed ball milling, *Green Chem.*, 2009, **11**, 1821.

50 C. G. Vogt, S. Grätz, S. Lukin, I. Halasz, M. Etter, J. D. Evans and L. Borchardt, Direct Mechanocatalysis: Palladium as Milling Media and Catalyst in the Mechanochemical Suzuki Polymerization, *Angew. Chem., Int. Ed.*, 2019, **58**, 18942–18947.

51 T.-X. Métro, J. Bonnamour, T. Reidon, A. Duprez, J. Sarpoulet, J. Martinez and F. Lamaty, Comprehensive Study of the Organic-Solvent-Free CDI-Mediated Acylation of Various Nucleophiles by Mechanochemistry, *Chem. – Eur. J.*, 2015, **21**, 12787–12796.

52 C.-H. Chen, F. Mentink-Vigier, J. Trébosc, I. Goldberga, P. Gaveau, E. Thomassot, D. Iuga, M. E. Smith, K. Chen, Z. Gan, N. Fabregue, T.-X. Métro, B. Alonso and D. Laurencin, Labeling and Probing the Silica Surface Using Mechanochemistry and ^{17}O NMR Spectroscopy, *Chem. – Eur. J.*, 2021, **27**, 12574–12588.

53 C.-H. Chen, E. Gaillard, F. Mentink-Vigier, K. Chen, Z. Gan, P. Gaveau, B. Rebière, R. Berthelot, P. Florian, C. Bonhomme, M. E. Smith, T.-X. Métro, B. Alonso and D. Laurencin, Direct ^{17}O Isotopic Labeling of Oxides Using Mechanochemistry, *Inorg. Chem.*, 2020, **59**, 13050–13066.

54 (*a*) E. Boldyreva, Non-ambient Conditions in the Investigation and Manufacturing of Drug Forms, *Curr. Pharm. Des.*, 2016, **22**, 4981–5000; (*b*) A. A. L. Michalchuk, I. A. Tumanov, S. Konar, S. A. J. Kimber, C. R. Pulham and E. V. Boldyreva, Challenges of Mechanochemistry: Is In Situ Real-Time Quantitative Phase Analysis Always Reliable? A Case Study of Organic Salt Formation, *Adv. Sci.*, 2017, **4**, 1700132.

55 B. P. Hutchings, D. E. Crawford, L. Gao, P. Hu and S. L. James, Feedback Kinetics in Mechanochemistry: The Importance of Cohesive States, *Angew. Chem., Int. Ed.*, 2017, **56**, 15252–15256.

56 M. Carta, S. L. James and F. Delogu, Phenomenological Inferences on the Kinetics of a Mechanically Activated Knoevenagel Condensation: Understanding the "Snowball" Kinetic Effect in Ball Milling, *Molecules*, 2019, **24**, 3600.

57 J. Andersen, J. Brunemann and J. Mack, Exploring stable, sub-ambient temperatures in mechanochemistry via a diverse set of enantioselective reactions, *React. Chem. Eng.*, 2019, **4**, 1229–1236.

58 C. Leroy, S. Mittelette, G. Félix, N. Fabregue, J. Špačková, P. Gaveau, T.-X. Métro and D. Laurencin, Operando acoustic analysis: a valuable method for investigating reaction mechanisms in mechanochemistry, *Chem. Sci.*, 2022, **13**, 6328–6334.

59 **https://mph.readthedocs.io/en/stable/**.

60 J. Špačková, C. Fabra, S. Mittelette, E. Gaillard, C.-H. Chen, G. Cazals, A. Lebrun, S. Sene, D. Berthomieu, K. Chen, Z. Gan, C. Gervais, T.-X. Métro and D. Laurencin, Unveiling the Structure and Reactivity of Fatty-Acid Based (Nano)materials Thanks to Efficient and Scalable ^{17}O and ^{18}O-Isotopic Labeling Schemes, *J. Am. Chem. Soc.*, 2020, **142**, 21068–21081.